

Octapartite parameterization for the spin- $\frac{1}{2}$ square lattice Heisenberg antiferromagnet

Bayo Lau, Mona Berciu, and George A. Sawatzky

Department of Physics and Astronomy, University of British Columbia, Vancouver, BC, V6T 1Z1

(Dated: November 18, 2018)

We introduce a novel parameterization of the Hilbert space of a spin- $\frac{1}{2}$ Heisenberg antiferromagnet using an octapartite description of the square lattice. This provides a systematic way to model the ground-state wavefunction within a truncated basis. To prove its effectiveness we study systems with up to 64 spins using exact diagonalization. At significantly reduced computational cost, we get ground-state energies within 1% of the best published values. Its non-iterative nature and lack of exploitation of spatial symmetries make this approach suitable for generalization to doped systems.

Introduction: The discovery of the high- T_c cuprates has emphasized the need to understand the physics of charged fermions moving in a two-dimensional (2D) background of antiferromagnetically (AFM) coupled spins, as represented by a doped Hubbard model.¹ Since an analytical solution seems unattainable, numerical modeling of large-scale, strongly correlated doped systems is of extreme importance and has been pursued in many different ways, each with their own advantages and disadvantages.

For example, the powerful Monte Carlo (MC) methods give extremely accurate information for the undoped AFM, providing the benchmark for the ground state (GS) energies and correlation functions of systems with up to thousands of spins.² However, they are limited by the sign problem if additional fermions are present. This lead to work on alternative optimized ways for treating the undoped AFM, with the latest development in MC sampling being the use of variational RVB-type ansätze.³⁻⁵ In the same context, density matrix renormalization group (DMRG) has also progressed over the years.⁶

Since the interactions with the fermions are often comparable or bigger than the AFM's energy scale, most such AFM-specialized methods require very non-trivial modifications to adapt to doped systems, due to technicalities of the RVB ansatz or the DMRG special boundary conditions. In fact, recent studies of doped systems still perform exact diagonalization (ED) of the full Hilbert space rather than trying to take advantage of either of these schemes.⁷⁻⁹ ED studies have the huge advantage that they provide the GS *wavefunction*, from which any GS properties, including all correlation functions, can be calculated. This would make ED the numerical method of choice, were it not for the extreme restriction on the sizes of doped systems that can be currently treated.^{8,9}

A very different way to approach the doped systems is to start from a non-optimal AFM background description, like the classical Néel state.¹⁰ However, the strong quantum fluctuations leading to strong deviations from a Néel-like background are believed to be an essential part of the low-energy physics of the doped systems. It is therefore necessary to find accurate yet efficient ways to describe the AFM background, which can also be straightforwardly extended to the doped problem.

Here we present a novel way to model the GS wavefunction for the undoped AFM, with a high level of accuracy that can be systematically improved. It is so effective

that the $N = 64$ wavefunction can be calculated as a numerical vector in a systematic basis with a commodity computer. The method is formulated in the real-space basis of the square lattice with periodic boundary conditions, in which other interactions are defined naturally. Neither translational nor point-group symmetries are exploited. Thus, it can be used as an excellent starting point for studying doped models where these symmetries are broken, or as an efficient kernel for iterative methods, such as renormalization and quantum cluster theory.¹¹

We stress that the immediate goal is not to compete with the MC powerhouses in dealing with large undoped systems. Rather, our method provides a general insight in the essence of the AFM background, which can be used to then reduce the computational cost for larger doped systems with only slight loss of accuracy. Availability of such efficient yet accurate methods is invaluable in allowing extensive studies of dependence on various parameters, to shed light on their importance and effects.

In this paper we discuss the physical insights behind our method and apply it to the undoped AFM, where its accuracy can be easily gauged. Application to doped models is in progress and will be presented elsewhere.¹³ With the AFM exchange taken as the energy unit, a N -site AFM Heisenberg model on a square lattice reads

$$H_{AFM} = \sum_{\langle i,j \rangle} \bar{S}_i \cdot \bar{S}_j. \quad (1)$$

The dimension of the Hilbert space is 2^N , and that of the commonly used $S^z = 0$ basis for the GS is $N! / (\frac{N}{2}!)^2$. It is the sheer size of the Hilbert space that makes this problem so difficult, and stimulates new approaches.

The method: After Anderson pointed out the connection between RVB states and the projected BCS-type wavefunction,³ the RVB framework has been implemented for an AFM torus by two approaches. The bottom-up route consists in the explicit optimization of the bond amplitudes.⁴ The top-down approach is the optimization of projected wave functions,⁵ (this showed the coexistence of superconducting and AFM order parameters for underdoped cuprates). So long as the AFM order parameter is finite, there should be another way to describe the wavefunction without the projecting ansatz or the micro-managing of bond amplitudes.

One way to specify a singlet with finite AFM order is

to divide the bi-partite lattice into sublattices A and B, and perform angular momentum addition between their states. If these states are classified by their total and z -projection quantum numbers, $S_{A/B} \in [0, \frac{N}{4}]$, $m_{A/B} \in [-S_{A/B}, S_{A/B}]$, we can build $S = 0$ singlet states:

$$|0, 0\rangle = \sum \frac{(-1)^{S_A - m_A}}{\sqrt{2S_A + 1}} \delta_{S_A, S_B} \delta_{m_A, -m_B} |S_A, m_A, S_B, m_B\rangle \quad (2)$$

The Hilbert space contains a huge number of such singlets. Since the AFM ground-state is also a singlet,¹⁴ if we label all possible singlets of Eq. (2) with an index α , we can express the GS wave function as their linear combination $|GS\rangle = \sum_{\alpha} c_{\alpha} |0, 0\rangle_{\alpha}$. We seek such an orthonormal basis which is also computationally efficient.

The staggered magnetization is a well-studied observable of the ground-state wave function. For a bi-partite lattice in a staggered magnetic field, this quantity is formally defined as the difference between $\langle m_A \rangle$ and $\langle m_B \rangle$ in the zero-field limit. In the absence of a staggered field, this quantity has alternative definitions, such as:

$$\hat{m}^2 = \frac{1}{N^2} \left(\sum_r (-1)^{|r|} \hat{S}_r \right)^2 = \frac{(\hat{S}_A - \hat{S}_B)^2}{N^2}, \quad (3)$$

where $\hat{S}_{A/B}$ are the total sublattice spin operators. In the AFM GS, $m = \langle \hat{m}^2 \rangle^{\frac{1}{2}}$ has been extrapolated to ~ 0.3 as $N \rightarrow \infty$, and increases like $1/\sqrt{N}$ to ~ 0.45 for $N = 32$.¹⁶ In terms of the total spin $\hat{S} = \hat{S}_A + \hat{S}_B$, we have:

$$\hat{m}^2 = \frac{1}{N^2} (2\hat{S}_A^2 + 2\hat{S}_B^2 - \hat{S}^2) \quad (4)$$

The ground state is a singlet, $S = 0$. It follows that the wave function must allocate significant weight to sectors with high values of $S_A = S_B$ in order to yield such large values of m . In fact, for the RHS of Eq. 4 to be larger than the expected value, the sublattice spins $S_{A/B}$ have to be within $\frac{N}{16}$ of their maximum values. Our computational basis takes advantage of this observation. There are many ways to add spins quantum mechanically, but not all are viable because the truncation error needs to be bounded systematically and the computational effort must be small. There are two extremes: if the original single-site basis of Eq. (1) is used, no basis transformation is needed but enforcing truncation based on Eq. (4) is costly. However, if a random basis tabulated according to values of S_A is used, transforming Eq. (1) into the new basis would be costly due to the many Clebsch-Gordan series needed. We propose a parametrization which is a good compromise between these two extremes.

Starting from the case where all $\frac{N}{2}$ sublattice spins add to the maximum of $\frac{N}{4}$, if we want to include states with spin down to $\frac{3N}{16} = \frac{N}{4} - \frac{N}{16}$, the basis must allow many new configurations, including ones where $\frac{N}{8}$ spins have a total spin of 0 while the other $\frac{3N}{8}$ spins have a total spin of $\frac{3N}{16}$. This suggests that groups of $\frac{N}{8}$ or fewer spins

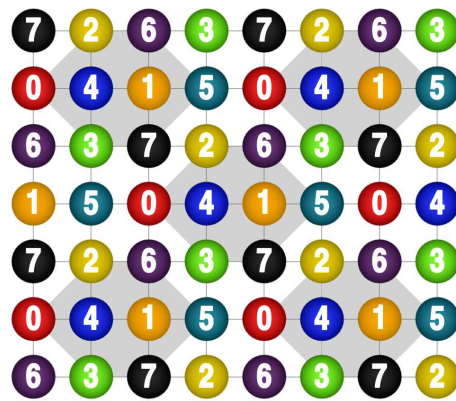


FIG. 1: (color online) Square lattice divided in octads (shaded areas). Sites positioned similarly inside octads have the same label. Each is surrounded by neighbors with different labels.

must be allowed to take *all* possible spin quantum numbers. Since a larger group would overshoot the sublattice spin below the $\frac{3N}{16}$ "threshold", while a smaller group would introduce extra "enforcement" costs as discussed above, we divide the full lattice into groups of 8 sites, see Fig. 1. The resulting *octads* repeat periodically with translational vectors $2a(1, \pm 1)$. Each spin is identified by the octad it belongs to, and by its position inside the octad. A sublattice is composed from 4 groups of spins indexed with the same label, *e.g.* $\hat{S}_A = \hat{S}_0 + \hat{S}_1 + \hat{S}_2 + \hat{S}_3$. With this arrangement, each spin interacts with spins from all the 4 groups of the other sublattice, *e.g.* a group 0 spin is always to the west/east/south/north of a spin in group 4/5/6/7. This partition is the minimum division that permits such a description and is a fundamental building block for the wave function in the model. Even though we arrived at it by looking to optimize the computation, our partition has been used in other contexts.¹⁵

We now straightforwardly generalize Eq. (2) and write singlets of the total lattice as:

$$|0, 0, f(\{S_i\})\rangle = \sum c_{\{S_i, m_i\}} \prod_{i=0}^7 |S_i, m_i\rangle \quad (5)$$

where S_i, m_i are the quantum numbers for \hat{S}_i , *i.e.* the total spin for group $i = 0, 7$. Here, $c_{\{S_i, m_i\}}$ is the product of the appropriate Clebsch-Gordan coefficients for the 8 pairs of quantum numbers (S_i, m_i) . The $f(\{S_i\})$ index on the LHS keeps track of the many ways in which these spins can be added to form a singlet.

If all these singlets are kept into the computational basis, the GS calculation is exact. The total spin of each group takes values $S_i \in [0, \frac{N}{16}]$, and there is no reason to restrict them. However, our previous discussion suggests that while all possible S_i values must be allowed, the singlets with highest GS weight are those whose total sublattice spin is within $\frac{N}{16}$ of the maximum value.

We therefore parameterize the singlet Hilbert space in terms of a completeness parameter, $C_s \in [0, 1]$, and in-

clude in the singlet basis only states for which $S_{A/B} \geq \frac{N}{4}(1 - C_s)$. For $C_s = 1$, the calculation is thus exact. For $C_s = \frac{1}{4}$, this means that the maximum number of anti-aligned spins in the sublattice is $\frac{N}{8}$. Based on the discussion for the staggered magnetization, we expect this to already be a good variational basis for the GS. For any $C_s \neq 1$, this formulation allows *all possible values* of S_i for each $i = 0, 7$, but restricts the ways in which they can combine to give the total sublattice spin. The number of degenerated states is combinatorially large due to the large degeneracy of states with low sublattice spins.

Eq. (5) is invariant under spin rotations, thus the anti-alignment is enforced here in terms of angular momentum addition, very different from the classical Néel picture. This approach also maintains the full translational symmetry of the Hamiltonian. If the RVB bond-amplitude optimization is a bottom-up way of adding AFM order to a singlet,⁴ our method is a compatible top-down approach without the need of projecting an ansatz.

The cost of this truncation scheme is the one-time computation of matrix elements between these basis states. This is acceptable because conventional diagonalization schemes are limited by storage, not processor speed, and this data is reusable for other computations that involve the AFM. The octapartite division of Fig. 1 is valuable for greatly minimizing the number of finite matrix elements of the Hamiltonian in the basis states of Eq. (5). The two-body interaction can be computed efficiently because only 2 out of 8 kets in Eq. (5) are changed and the delta functions in the Clebsch-Gordan coefficients of Eq. (5) allow data to be aligned in a computationally efficient way. The overall matrix can be constructed column-by-column and term-by-term and is extremely sparse. The practical implication is that the grand problem is decomposed into many small independent computations which can be massively parallelized. Table I compares the $C_s = \frac{1}{4}$ basis size to those of other bases commonly used by non-iterative methods. At $C_s = \frac{1}{4}$, the $N = 32$ system was solved within seconds using a generic Lanczos routine. Even for the 9.8×10^8 -size basis for $N = 64$, the GS vector can be calculated with a power method using less than 15 matrix-vector products, each taking less than 30 minutes with a single cpu thread on a xeon workstation. Another advantage is the absence of the gapless $S = 1$ magnon excitations from the variational space, which allows the matrix-vector products to converge rapidly. Since these excitations are Goldstone modes, the required $S = 1$ basis to describe them has roughly the same size as the

TABLE I: Size of the $C_s = \frac{1}{4}$ subspace as compared to that of the commonly used basis.

N	$C_s = \frac{1}{4}$	$S = 0$	$S_z = 0$	Full
16	50	1430	12870	2^{16}
32	11041	35357670	601080390	2^{32}
64	9.8×10^8	5.55×10^{16}	1.83×10^{18}	2^{64}

$S = 0$ basis required for the GS, and can be generated by appropriately changing the Clebsch-Gordan coefficients in Eq. (2). The modeling of *collective* magnon excitations in the presence of carriers is model-dependent and will be discussed elsewhere.¹³

Results: We have performed computations for the full basis for $N = 16$ as a benchmark for larger N values. For $N = 32$ (64) we computed up to $C_s = \frac{1}{2}$ ($C_s = \frac{1}{4}$). While the computations with $C_s < 1$ are variational, the goal here is to demonstrate that $C_s \sim \frac{1}{4}$ is a good rule-of-thumb value to capture well the AFM ground-state.

The stability of this formulation is demonstrated in Fig. 2(a) which shows the overlap between the GS wave functions for consecutive values of C_s . The deviation decreases exponentially with increasing C_s , and for $C_s = \frac{1}{4}$ the overlap is $\approx 95\%$. We conclude that the GS vector is already pointed in the correct direction even for small C_s , and subsequent increments of C_s merely result in minor improvements. This is reinforced by the convergence of the GS energy demonstrated in Fig. 2(b), which supports the scaling law $\frac{dE_{GS}}{dC_s} \sim e^{-\alpha C_s}$. The error decays exponentially, with a rate that increases with N . The $N = 32, 64$ lines cross at $C_s \sim \frac{1}{4}$ where the fractional error is $\sim 10\%$. This exponential efficiency is amplified by the fact that a linear decrease in C_s leads to a combinatorial decrease of the basis size because of the numerous low-spin combinations removed from the basis.

These GS energies are not as accurate as for established iterative methods, however a single-pass computation at $C_s = 1/4$ already has less than 2% error. Using a linear fit of $\frac{dy}{dx} \sim e^{-x}$, an estimate of E_{GS} at $C_s = 1$ is obtained by simple integration (see Fig. 3). From the $C_s = 1$ estimates and the $N^{-\frac{3}{2}}$ scaling, we extrapolate $\lim_{N \rightarrow \infty} \frac{E_{GS}}{N} = -0.6671$, within 0.5% of the best published value of -0.6692,¹⁶ even though it is achieved at a significantly reduced computational cost.

We have thus far demonstrated the exponential convergence of the GS eigenvalue and eigenvector with increasing C_s , which validates our proposed variational basis.

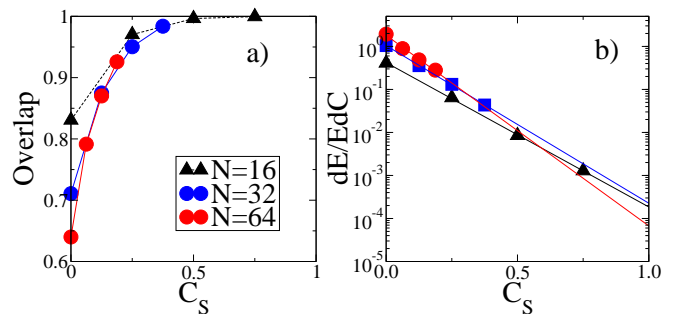


FIG. 2: (color online) (a) Overlap $|\langle GS, C_s | GS, C_s + \frac{2}{N} \rangle|^2$ between ground-state wave functions corresponding to adjacent values of C_s for $N = 16, 32, 64$. Note that for $N = 64$, the overlap is already 95% for $C_s = \frac{1}{4}$; (b) Fractional change $\frac{1}{E_{GS}} \frac{dE_{GS}}{dC_s}$ in ground-state energy corresponding to different C_s cutoffs. The lines are linear fits to the data.

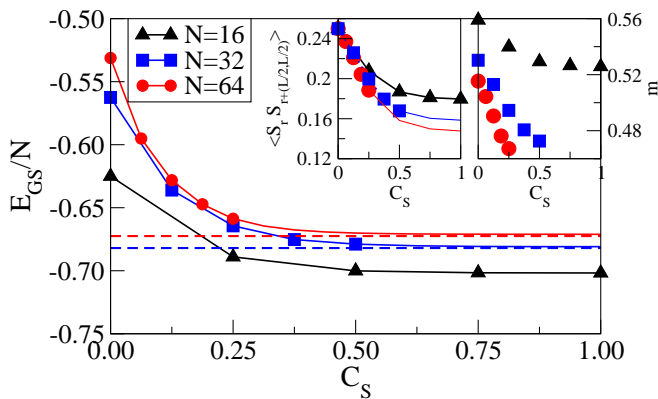


FIG. 3: (color online) GS energy computed at specific C_s values (symbols) and the extrapolation to $C_s = 1$ (solid lines) for $N = 16, 32, 64$. The horizontal dashed lines are the lowest values from Ref. 16. Inset: expectation values of the non-commuting operators $\sqrt{\langle m^2 \rangle}$ and $\langle \vec{S}_r \cdot \vec{S}_{r+(\frac{L}{2}, \frac{L}{2})} \rangle$.

Because MC studies cannot produce an explicit wavefunction, they often gauge accuracy via spin-spin correlation operators which do not commute with the Hamiltonian. The insets of Fig. 3 show expectation values of two such operators (the staggered magnetization of Eq. 4 and the spin-spin correlation at maximum distance) evaluated from our eigenvector for a given value of C_s . Although these operators are non-commuting, their matrix representation is diagonal in our basis and therefore trivial to compute. The convergence of these quantities is essentially linear for $C_s < \frac{1}{4}$. For greater values of C_s , $\frac{d}{dC_s} \langle \vec{S}_r \cdot \vec{S}_{r+(\frac{L}{2}, \frac{L}{2})} \rangle$ is suppressed faster than $\sim e^{-C_s}$ so the post-threshold convergence is even better than for the GS energy. On the other hand, because m is exploited to discard low-spin parts of the Hilbert space, its approximated value is always higher than the true value; convergence is only asymptotical for $C_s > \frac{1}{4}$. Thus, the computational discount for the GS wavefunction at a small C_s is achieved at the cost of lowered accuracy

for one of many definitions of staggered magnetization, which does not commute with \mathcal{H}_{AFM} .

Conclusions: We introduced an octa-partition of the square lattice, and used it to build an orthonormal singlet basis for calculating the AFM GS. We used C_s to systematically parameterize the resulting Hilbert space, and proposed apriori arguments to postulate that $C_s \sim \frac{1}{4}$ is the minimal value that captures the GS accurately. The resulting basis is combinatorially smaller than in any other schemes, apriorily known, and computationally very efficient. We demonstrated the stability of the formulation in Fig. 2(a) and identified the sources of error. Using a single thread on a commodity computer, single-pass matrix computations are feasible for systems with up to $N = 64$ spins, significantly exceeding the current full ED record of $N = 40$.⁹

While other established methods can yield smaller errors for the GS for larger N values, they cannot be easily generalized. Our formulation is non-iterative and is defined in the real space coordinate of a torus without exploiting spatial symmetries. This allows for an economic generalization of this approach into iterative procedures.

One concern about Hilbert space truncation is its applicability to complicated models. Our formulation by itself does not involve MC sampling and so it is not subject to the sign problem. One outstanding issue in cuprates is the explanation and measurement of the photoemission spectrum at low doping and low temperature.¹⁷ Information about the spectrum is contained in the Krylov space of the model Hamiltonian acted on the AFM GS;¹⁸ thus, a compact description of the AFM GS in a systematic orthonormal space can indeed narrow the space spanned by calculations. Because the total spin of the AFM plus carriers is conserved while AFM order is expected to persist for low doping at low temperature, our method can be generalized to reduce the Hilbert space of the doped systems. The details are model-dependent and outside the scope of this paper; this work is progress.

Acknowledgement: This work was supported by NSERC, CIFAR and CFI.

¹ P.A. Lee, N. Nagaosa, X.G. Wen Rev. Mod. Phys. **78**, 17 (2006); P.A. Lee, Rep. Prog. Phys. **71**, 012501 (2008).
² J.D. Reger, *et al.*, Phys. Rev. B **37**, 5978 (1988); H.G. Evertz, *et al.*, Phys. Rev. Lett. **70**, 875 (1993); A. Sandvik, Phys. Rev. B. **59**, R14157 (1999); W. Foulkes *et al.* Rev. Mod. Phys. **73**, 33 (2001); F. Mezzacapo, *et al.* arXiv:0905.3898 (2009).
³ P. W. Anderson, Science **235**, 1196 (1987).
⁴ S. Liang, *et al.*, Phys. Rev. B **61**, 365 (1988); J. Lou, *et al.*, Phys. Rev. B **76**, 104432 (2007).
⁵ A. Himeda, *et al.*, Phys. Rev. B **60**, R9935 (1999); D. A. Ivanov, Phys. Rev. B **70**, 104503 (2004); S. Sorella, Phys. Rev. B **71**, 251103 (2005); M. Ogata, *et al.*, Rep. Prog. Phys. **71** 036501 (2008).
⁶ S. R. White, *et al.*, Phys. Rev. Lett. **99**, 127004 (2007); S. R. White *et al.*, Phys. Rev. B **79**, 220504R (2009).

⁷ A. Luscher, *et al.*, Phys. Rev. B. **79**, 195102 (2009).
⁸ P. W. Leung, Phys. Rev. B. **73**, 075104 (2006).
⁹ J. Richter, *et al.*, in Quantum Magnetism, Lecture Notes in Physics 645 (Springer, Berlin, 2004), p. 85.
¹⁰ J. Bonca, *et al.*, Phys. Rev. B. **76**, 035121 (2007).
¹¹ T. Maier *et al.*, Rev. Mod. Phys. **77**, 1027 (2005).
¹² D.D. Betts, *et al.*, Can. J. Phys. **77** 353 (1999); A.L. Chernyshev, *et al.*, Phys. Rev. B **58** 13594 (1998).
¹³ B. Lau *et al.*, unpublished.
¹⁴ W. Marshall, Proc. Roy. Soc. (London) A232, 48 (1955).
¹⁵ C. Brugger *et al.*, Phys. Rev. B **74**, 224432 (2006).
¹⁶ E. Manousakis, Rev. Mod. Phys. **73**, 1 (1991).
¹⁷ F. Ronning *et al.*, Phys. Rev. B **67**, 165101 (2003).
¹⁸ A. Damascelli, *et al.*, Rev. Mod. Phys. **75**, 473 (2003).